PACS №: 84.30.Jc

Bruce L. Freeman[+], Larry L. Altgilbers[++], C. Maxwell Fowler[+++] and Alvin D. Luginbill
[+] Texas A&M University, TAMUS-3133
College Station, TX 77843-3133 USA
E-mail: bruce.freeman@ne.tamu.edu
[++] Advanced Technology Directorate,
US Army Space and Missile Defense Command
[+++] Los Alamos National Laboratory and
Texas A&M University Adjunct Professor,
Nuclear Engineering

Similarities and Differences between Small FCG'S and Larger FCG'S*

Contents

Abstract

After experimentally testing eight different designs of small explosive-driven, magnetic flux compression generators (FCGs), several similarities and differences have emerged when compared to larger FCGs. While the similarities were expected, the differences are rather surprising. The magnetic flux compression generators under consideration are small. Their armature diameters range from 0.95 cm to 2.54 cm.
The similarities and differences are discussed using three figures of merit; alpha, magnetic flux efficiency, and energy gain. Experimental information is provided from tests of the small generators.

1. Introduction

Of the various geometries available for magnetic flux compression generators (FCG), the one most used is the helical variant of the FCG (Figure 1). The reason for this selection is because this style of generator generally has higher current and energy gains into larger inductive loads than other FCG configurations. However, the helical FCG is also the most complicated generator to either build or understand. In fabrication, an unsupported, precision solenoidal winding is constructed. In turn, this winding must be very carefully positioned with respect to the centerline, relative to the armature to avoid the more obvious clocking or turn skipping flux losses. The challenge is significant for the larger systems, but this can become a daunting task for the smaller FCGs. The physics of the helical generator is both fascinating and not completely understood. For example, magnetic flux loss in any FCG will limit its performance. In a cylindrical geometry, the generator performance can be and has been calculated essentially from first principals. In contrast, the geometry and action of a

*This work is solely funded by the Explosive-Driven Power Generation MURI program funded by the Director of Defense Research & Engineering (DDR&E) and managed by the Air Force Office of Scientific Research (AFOSR).

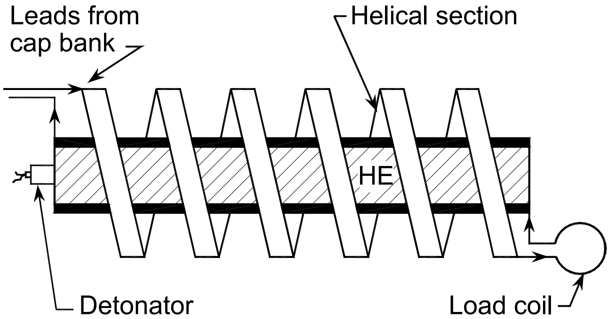

Fig. 1. The helical FCG, before HE initiation, has a cylindrical armature and a solenoidal stator, which provides much larger initial inductance than other geometry FCGs.

helical FCG is sufficiently complex that the authors are not aware of any calculation that does more than approximate performance, always with an adjustment available within the code to enable tweaking between computed results and experimental results. One important area within a helical FCG that needs more study is the armature-stator contact mechanics and a detailed understanding of how the current actually transfers between the two in the moving contact region. The physics of this current transfer is not well understood, particularly as the rotation frequency increases. Also, what is the degree of current crowding that occurs in the stator winding as the armature approaches to within a scale distance of closure? Another question involves the magnetic field rotation that typically occurs through the generator output section. Within the helical generator the magnetic field is essentially axial. In the output section, the current is typically axial, and the magnetic field has been rotated to the azimuthal direction. Thus, the question may be either whether the $\nabla \times \mathbf{B}$ or the $\mathbf{E} \times \mathbf{H}$, Poynting flux, rotation poses a limitation on the operations of these FCGs.

Since these and many related issues are indeed very complex, the typical approach within the flux compression community is to adopt one or a few figures of merit for the assessment of FCG experimental performance [1]. If one defines for a helical FCG the initial current, I_0, the final current, I_f, the initial generator inductance, L_G, and the load inductance, L_l, a practical measure of these generators can be expressed in terms of a, where this quantity is defined by the *current gain*, G_I:

$$G_I = \left(\frac{I_f}{I_0}\right)_{Experimental} = \left(\frac{L_G + L_l}{L_l}\right)^{\alpha}_{Ideal}, \quad (1)$$

where the subscripts refer to the theoretical or ideal gain compared to the experimental performance and the resistance of the circuit is assumed very small. A second consideration is the flux conservation of a given generator design into a fixed inductance load. The figure of merit is simply the percentage of magnetic flux retained within the generator system and is given by the *flux efficiency*, F_E;

$$Flux\,Efficiency = \frac{(L_l I_f)}{((L_G + L_l)I_0)} \times 100\,\%, \quad (2)$$

or cast into the same representation as the definition of the α parameter, this equation becomes

$$Flux\,Efficiency = \left(\frac{L_G + L_l}{L_l}\right)^{\alpha-1} \times 100\,\%, \quad (3)$$

A third figure of merit that we use is the *energy gain*, G_E, which is more demanding of generator performance than the current gain. If the initial energy is E_0 and the final energy is E_f., the ideal energy gain is:

$$Energy\,Gain_{Ideal} = \frac{E_f}{E_0} = \left(\frac{L_G + L_l}{L_l}\right). \quad (4)$$

For experimental comparisons, the parameter, a, may be used again, so the ideal equation becomes

$$Energy\,Gain_{Experiment} = \frac{\frac{1}{2} L_l I_f^2}{\frac{1}{2}(L_G + L_l) I_0^2} = \left(\frac{L_G + L_l}{L_l}\right)^{2\alpha-1}. \quad (5)$$

In all of these considerations, the transmission line inductance has been taken to be part of the generator's inductive load and resistance has been neglected.

In the past, the groups using the larger flux compression generators have been able to refine the geometries to the point where the helical systems are predicted reasonably well. More recently, there has been a growing interest in the use of very small helical FCGs in compact systems. Therefore, the questions concerning the relative performance of these very small generators are becoming keys to whether these units will be useful in the anticipated applications requiring small generators as power supplies. Thus far, our group has observed that the very small helical FCGs act, in some instances, differently from what one would expect with the larger generators, as noted by others [2].

In the discussions of relative performance of the smaller generators, two styles of the Texas A&M University (TAMU) experimental FCGs will be presented. The first is the TAMU Mark 101. This generator uses a 2.54-cm diameter armature with a 12^0 tapered-stator winding. Thus, the armature expands by about a factor of two at the input glide plane before completing its final expansion as a phased closure with the stator winding. The explosive loading for this unit is about 120 grams of Composition C-4 explosive. The development of this and related

Table 1. Sandia standard generator [2]

Inner Coil Radius	15.25 mm
Outer Armature Radius	7.95 mm
Wire Diameter (Cu)	0.40 mm
Coil Length	32 mm
Number of Turns	70
Average Cone Angle	11.5^0
Magnetic Reynolds Number	1150

generators is discussed in a companion paper [3]. The second generator used in this discussion is the TAMU Mark III. This simple helical FCG has a 0.95-cm diameter armature and a 1.91-cm diameter stator. It has proven to be a useful test bed for examining several issues involved with the very small units. As is evident from the data presented, the degree of difficulty for the fabrication and assembly precision required to avoid turn skipping is significantly more than for the TAMU Mark 101. However, at this scale size neither generator is straightforward.

2. Previous Small FCG Studies

There have been relatively few studies dedicated to the study of small helical FCGs. Probably the first theoretical [4] and experimental [2] study that focused on small ($\sim$ 100 cm^3) FCGs was done at Sandia National Laboratories. They investigated a helical FCG in which the coil was closely wound with as many as 100 turns of thin (1 mm or less) wire. These generators were different than the other contemporary generators in that they generated much less energy, only a few hundred joules, and had much closer spacing between the turns of the coil, higher wiping velocities at the contact, and ability to handle much higher inductive loads. Sandia conducted more than 150 tests of their "standard" FCG (see Table 1). There was considerable scatter in the electrical data due to mechanical issues; mainly controlling mechanical tolerances. To improve the performance of these generators, the following recommendations were made: reduce mechanical tolerances, improve armature design, and identify new insulating materials that have good high voltage hold-off capability under normal conditions but undergo rapid breakdown under mechanical shock.

Later, work was done at the Lawrence Livermore National Laboratory (LLNL) by Abe and Chase [5]. These generators were used to help benchmark a computer simulation [6,7]. This generator was characterized by having small volume (< 600 cm^3), close spacing of the stator turns, relative high armature/stator contact velocity, and high current multiplication factor. The generator had an inductance of 74.5 μH and DC resistance of 0.7 Ω. The stator had an inner diameter of 5.1 cm and overall length of 5.1 cm. It was wound with #24 copper magnet wire in four stages. The first stage was a simple helix of 37 turns with a pitch of 15.75 turns/cm. The second stage is bifurcated with two parallel turns of 6 and 6.5 turns at a pitch of 7.875 turns/cm. The third stage is further bifurcated into four parallel helices with a pitch of 3.94 turns/cm. The final stage bifurcated into 8 parallel helices with a pitch of 1.97 turns/cm. The stator had a layer of Kapton dielectric to insulate it from the armature. The armature was made of copper, had a length of 8.04 cm, and tapered at a 4 degree angle 4.13 cm from one end. Three loads were tested: short circuit, constant resistance, and constant inductance. They found that the performance of the generator is inversely proportional to the load impedance. This result stressed the importance of matching the load to the generator for optimal performance.

Similar studies were conducted in Russia by A.B. Prishchepenko [8] and Demidov [9]. Prishchepenko tested a series of FCGs ranging in diameter from 36 to 50 mm and some of the results are presented in Table II. V.A. Demidov et al [9] tested the EMG-50CL generator which had a stator with a length of 200 mm and inside diameter of 50 mm with a conical output liner. They have demonstrated it is possible to use this compact generator with either a conical liner or a conical stator to power high impedance loads through an electro-explosive opening switch. They have used piezoelectric generators to seed the EMG-50CL [10].

Brooker, Manton, and McKay [11] in the United Kingdom developed two types of small generators. Both of these generators had a 30-mm diameter aluminum armature filled with 0.25 kg of PE4 explosive. The coil of one version was hand wound, while the other was precision machined for greater accuracy of alignment. The hand-wound coil had a length of 20 cm and was wound with 2.64 mm round copper wire insulated with heat shrink sleeving. Its performance was erratic due to turn skipping caused by misalignments. The flux efficiency dropped with an increase in seed current and ranged from 23 % when the initial current was 1 kA, to 16 % when the initial current was 4 kA, and to 11.3 % when the initial current was 9 kA. The current and energy gains ranged from 20 and 13.8, to 9.7 and 4.6, and to 2.2 and 1.1 for the respective seed currents. The machined FCG stator consisted of 27 constant-pitch turns machined from a copper cylinder and had a width of 4.4 mm. The coils were potted in epoxy resin and the resin inside the coil was machined out. Their flux efficiency increased from 12.8 % to 19.2 % as the seed current increased from 5.2 kA to 10 kA.

Table 2. Prishchepenko's small FCGs [8]

Stator Diameter (mm)	Stator Length (mm)	Initial Inductance (μH)	Initial Energy (J)	Final Inductance (μH)	Final Current (kA)	Flux Conservation	Armature Geometry
36	40	12	3.0	20	68	0.14	Tapered
50	50	20	4.0	50	56	0.22	Tapered
50	70	100	2.9	25	97	0.1	Cylindrical
50	70	120	3.0	25	99	0.093	Cylindrical
50	100	115	2.8	25	148	0.15	Cylindrical

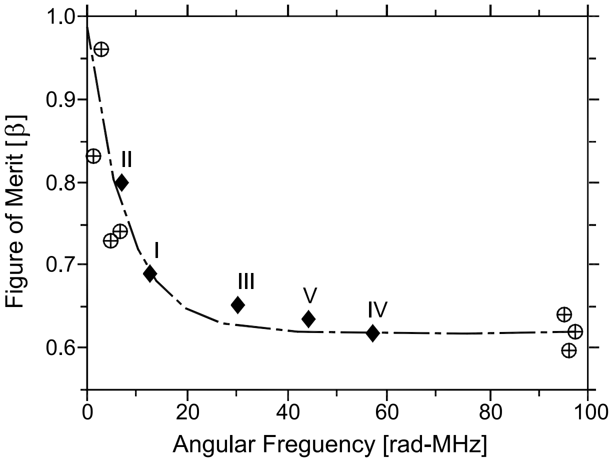

Fig. 2. Dependence of the figure of merit on the contact point's angular frequency for FCGs with constant diameter armature and single stage design. Data points are calculated from experimental data in references [Gov79], [Leh99], [Nov95], [Fow89], [Jon79], [Fre79], circle symbols, and own tests, diamond symbols. The solid line serves as guide for the eye only. Indicated are the authors' [Neu01] generators: TTU I

The current gain increased from 9.4 to 14.2 and the energy gain from 0.115 to 2.7. The lower efficiency of the machined-stator FCGs is thought to be due to voltage breakdown as a result of the lack of insulation between the coil and the armature [12].

More recently, Texas Tech University (TTU) has built and tested several variations of their "standard" helical FCG including constant diameter armature and stator, tapered armature, and tapered stator generators. The focus of their program was to identify and mitigate those physics related issues that impacted the efficiency of the generators. In one set of experiments [13], they built and tested two single wire, constant pitch generators that only differed in the separation of the stator and armature. In both cases, the outside diameter of the armature was 1.5 inches [38.1 mm], while the stator diameter was 2.6 inches (TTU I) [66.0 mm] in one case and 3.5 inches (TTU II) [88.9 mm] in the other case. In order to compare the impact of these size differences on operation of the generator, the angular frequency, ω of the azimuthally moving contact point was introduced. Assuming a simple equation for the inductance of a long solenoid with closely spaced turns, the following equations can be written:

$$\begin{aligned} L &= \mu_0 \frac{\pi(x^2-1)}{4} N^2 \frac{d^2}{l}, \\ \omega &= 2\pi v_0 \frac{N}{l}, \\ V &= \frac{\pi(x^2-1)}{4} d^2 l, \end{aligned} \tag{6}$$

where L is the generator inductance, x is the expansion ratio, N is the number of turns, d the armature diameter, l is the length, v_0 the detonation velocity, and V the compressed volume between the armature and stator. Rearranging these equation, ω is:

$$\omega = \frac{2\pi v_0}{\sqrt{\mu_0}} \sqrt{\frac{L}{V}}. \tag{7}$$

Since ω is related to the rate of change in the magnetic field structure in the generator, it may provide insight about the anomalous losses in the generator. This possibility was examined by plotting ω versus the figure of merit α in Fig. 2. Note that as ω increases; that is, as the volume (or radius) of the generator decreases, the figure of merit decreases implying higher ohmic losses.

To understand these losses, TTU investigated a tapered modification of their simple constant diameter armature, inch-size generators [14]. They have observed two types of losses in FCGs: ohmic losses due to the finite resistance of wires and armature materials and intrinsic flux losses, which may be unrecoverable flux trapped in the conducting layers of the generator components and thus lost for compression. For these studies they used the TTU II, IV, and X generators. It was concluded

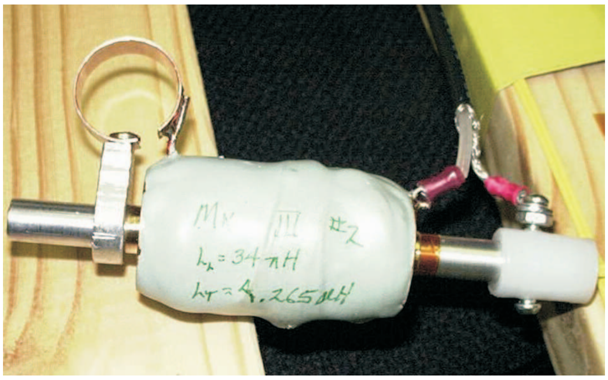

Fig. 3. TAMU Mark III generator just before being tested.

Fig. 4. TAMU Mark 101 and 301 tapered stator generators.

that the constant diameter FCGs exhibited more intrinsic than ohmic losses (69 % compared to 16 %, respectively), while the tapered generator with the same stator dimensions and tapered armature exhibited less intrinsic and more ohmic flux losses (13 % compared to 66 %, respectively).

3. TAMU Small Generators

Like TTU, TAMU has also studied several variations of a helical MCG. As noted earlier in this paper, the discussion is limited to the TAMU Mark III (Figure 3) and the TAMU Mark 101 (Figure 4). However, the other variants will provide us with some clues about the physics issues that effect the operation of the generators.

The Mark III is a helical generator with constant diameter stator. The armature has an outside diameter of 0.95 cm and the stator an inner diameter of 1.91 cm. It uses $\sim$ 8.5 g of C-4 explosive and a RP-501 EBW detonator. The stator consists of 29 turns of #14 gage, round cross section, magnet wire. The input and output glide plane forms a 10^0 angle with respect to the armature axis.

The Mark 101 is a tapered generator with a 120 stator taper. The armature had an outside diameter of 2.54 cm and the stator an inner diameter of 5.64 cm at one end and 3.02 cm at the other end. The armature was machined from 3031 aluminum with a final wall thickness of 0.76 mm. The stator consists of 29 turns of #14 gage, round magnet wire.

4. Similarities between Large and Small FCGs

The first and least surprising similarity between the larger and smaller generators is that larger wire size leads to improved performance. One reason for this improvement may be the lowering of the effective current density on the stator-winding conductor. Even though the current in a wire will tend to concentrate in a continuously smaller portion of its circumference as the armature approaches for contact, a larger wire size will still enable a lower current density during this phase of conduction. Another possibility is that the winding pitch of the stator winding is lengthened with the larger wire sizes. One aspect of an increased stator pitch is that typically the windings are spaced further apart or are physically wider. Thus, any tendency to skip turns because of armature misalignment or out-of-round condition is reduced. Flux trapping is also reduced. A second aspect is that if the turns are spaced further apart, any voltage breakdown probability from one turn to the next is reduced.

Using the smaller TAMU Mark III generators for testing this aspect, two FCGs were fired with nearly identical initial currents. There were differences due to the wider winding wire for the 12-gage stator, as opposed to the 14-gage stator. The initial inductance of the 14-gage generator was 4.18 μH versus 2.65 μH for the larger wire. The passive load inductor for the small wire unit was 105 nH, and the load for the larger wire generator was 125 nH. On the basis of this, the ideal gain for the 14-gage generator was the larger of the two systems. The initial currents for the two FCGs were 696 A and 632 A. Nevertheless, the 12-gage unit provided the better performance with an α of 0.58, a flux efficiency of 27 %, and an energy gain of 1.65. The similar figures for the 14-gage generator were an α of 0.54, a flux efficiency of 18 %, and an energy gain of 1.32.

On several occasions in larger generators, square cross section wire has been used for the winding of the stator, rather than the commonly used round cross section wire. In this paper, the continuously machined stator designs are excluded from discussion since they have other associated issues to consider. Initially, one might conclude that the use of square wire would in fact provide a better magnetic geometry for the stator and result in improved performance of the generator. Experimentally, this has not proven to be the case. In the case of the Mark V generators at Los Alamos, the round wire performed better than the square wire. There have been three mechanisms proposed to account for this degradation of generator performance when square wire is used. These are (1) voltage enhancement at the edges of the wire and associated turn-to-turn breakdown, (2) inability to force the square wire to lay flat in the winding mandrel, which could lead to enhanced turn skipping or clocking, and (3) differences in the current conduction area relative to the current contact with the armature. This last point stems from recognizing that in round wire, the current is concentrated onto a small fraction of the circular surface just before actual armature contact. Thus, the current flowing on a round wire does not have to geometrically redistribute as much as in the case of square wire at the time of armature contact.

Presently, the issue is not resolved, but we can add a new data point. The performance of the smaller generators is also degraded by the use of square wire in the stator winding. In our experience, the square wire did lay very well on the winding mandrel, so geometrical non-uniformities do not appear to play a role in this phenomenon, at least in the case of our smaller FCGs. Also, the voltages generated within the small generators do not approach the values at which one would expect a breakdown condition. With present data, the current redistribution near the instant when the current flows in a wider area and transfers to the armature, leading to higher flux loses, cannot be ruled out.

For this study, we used the TAMU Mark 101, tapered-stator generator, which has a 2.54-cm diameter armature. For test #1, 12-gage round magnet wire was used and for test #2, 12-gage square wire was used. The respective inductances were 11.31 μH and 10.5 μH. The loads were adjusted to provide roughly the same gain in each case. The measured currents for the two generators are shown in Figure51. For the round wire unit, we measured an a of 0.67, a flux efficiency of 32 %, and an energy gain of 3.15. For the square wire generator, the α was 0.60, the flux efficiency was 25 %, and the energy gain was 2.0. Thus, the round wire FCG performed better than the square wire unit.

Finally, increasing the load inductance to lower the ideal gain increases the performance figures of merit. The Los Alamos National Laboratory (LANL) Mark IX generator provides a good example of this behavior in the larger generators [15]. For a load inductance of 35 nH, the α of this FCG has been measured as 0.79. With a load inductance of 140 nH, the α was 0.85.

To examine the relative figures of merit, we conducted two experiments using the TAMU Mark III FCG to study the effects of lightly versus more heavily loaded smaller generators with tests #9 and #10, Fig. 6. The initial inductances of the generators were 4.185 μH and 4.280 μH, respectively. The initial currents were 348 A and 284 A, with load inductances of 346 nH and 75 nH. For shots #9 and #10 respectively, the α's were 0.53 and 0.39, the flux efficiencies were 30 % and 8.3 %, and the energy gains were 1.14 and 0.4.

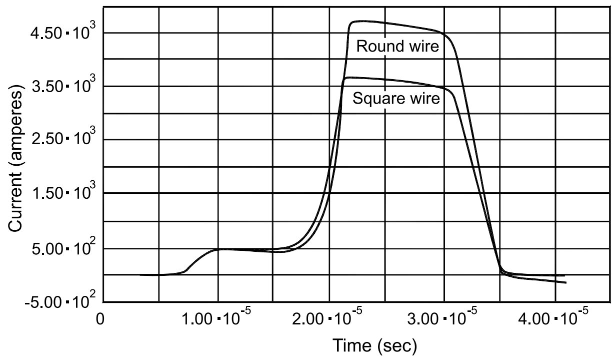

Fig. 5. Current traces from two Mark 101 tests show directly the differences in gain for round and square wire.

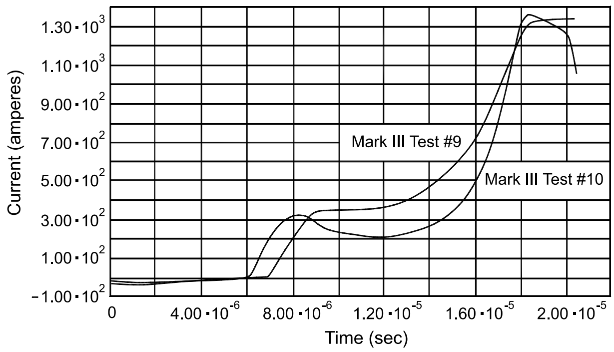

Fig. 6. The two current traces for the Mark III Test #9 and Mark III Test #10 are shown.

5. Differences between Large and Small FCGs

There are two significant differences between our smaller FCGs and the larger units. First, our small generators, so far, have demonstrated smaller gains than one might expect, given their ideal design gains, usually range from 10 to 50:1. In the larger FCGs, such as the LANL Mark IX, the generator gain is related to the ideal performance by an a of ranging from about 0.79 to 0.85, depending on generator loading. For the smaller FCGs, this figure of merit often ranges from about 0.5 to 0.6. From the defining equations, an FCG will not provide energy gain with an α less than 0.5. This issue may be explained simply by the existence of larger relative magnetic flux losses in the small

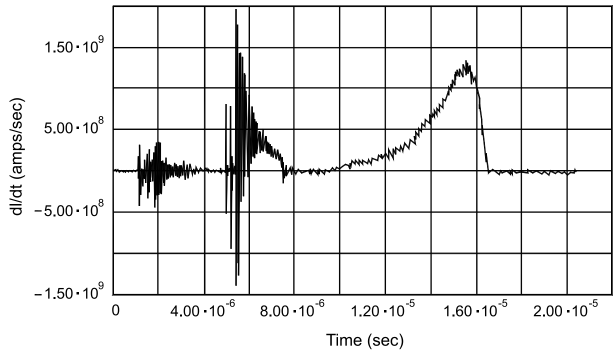

Fig. 7. The time derivative of the current for the Mark III Test #4 is shown.

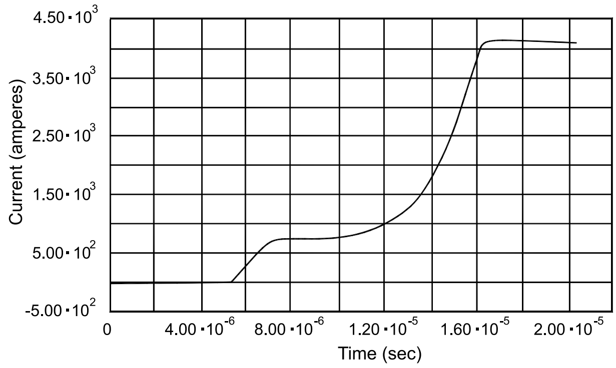

Fig. 8.
The current history for the Mark III Test #4 is shown.

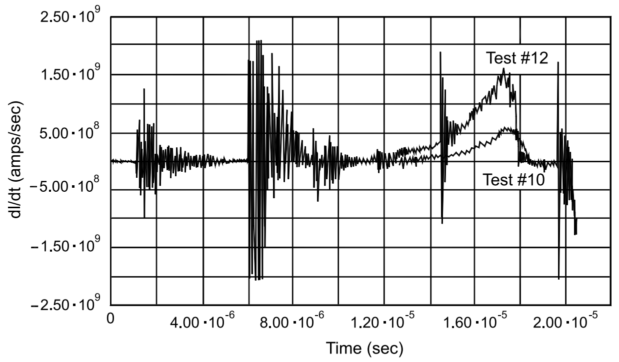

Fig. 9. The time derivative for the Mark III Tests #10 and #12 are shown for comparison.

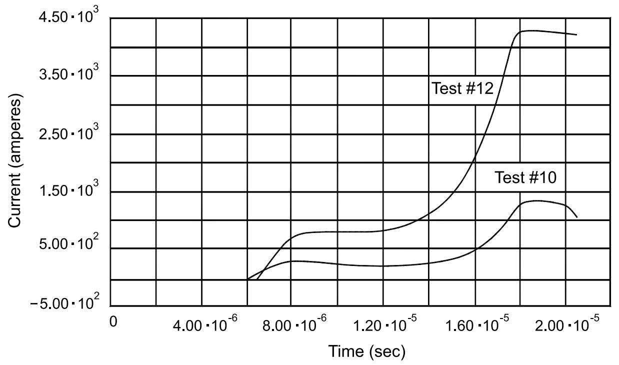

Fig. 10. The currents for the Mark III Tests #10 and #12 are shown.

FCGs. To a degree, these losses may be studied by modeling the hydrodynamic motions within the FCG as a function of time and by modifying the dynamics in the experimental systems to minimize potential flux pocketing.

For example, the fourth test of the TAMU Mark III generator is illustrated in Figures 7 and 8. The initial generator inductance was 4.16 μH with a passive load of of 234 nH. The initial current was 752 A with a final current of 4,140 A. The α for this experiment was 0.58, the flux efficiency was 29 %, and the energy gain was 1.61. The dI/dt plot in Figure 7 shows noticeable clocking or turn skipping behavior.

Second, increasing the initial current tends to result in better relative performance, until current density and saturation becomes an issue. In larger FCGs, higher initial currents lead to higher flux diffusion losses because the magnetic fields within the FCG are higher. From another viewpoint, any I^2R losses are enhanced. In our smaller systems, the higher initial currents increase the performance of the generator.

The results of the Mark III tests #10 and #12 will be compared (see Figures 9 and 10). These two generators were nearly identical with shot #10 having an initial inductance of 4.280 μH and shot #12 having an inductance of 4.100 μH. Further, the static load inductances were both 75 nH. The significant difference was that test #10 had an initial current of 284 A and test #12 had an initial current of 815 A. The figures of merit for the lower current test are an α of 0.39, a flux efficiency of 8.3 %, and an energy gain of 0.4. The higher current test, shot #12, had an α of 0.41, a flux efficiency of 9.4 %, and an energy gain of 0.49.

One possible explanation is that the lower kinetic energies in the small armatures do not result in as uniform a connection between the armature and stator as in the larger generators. Given such a phenomenon, any change in the initial conditions that would raise the internal voltage within the flux compression generator would possibly improve this connection process, resulting in an improvement in the figures of merit. Further research is needed to support or refute this hypothesis.

6. Summary

After testing many small explosive-driven magnetic flux compression generators with armature dimensions between 1.27-cm and 2.54-cm diameters, we have observed several similarities and differences relative to larger FCGs. Acknowledging that there are significant details of FCG performance that are not known in detail, it is necessary to use more generalized quantities or figures of merit to assess performance of the smaller generators. Three figures of merit have been used. These are the alpha defined by the relationship between the ideal and measured current gains in Eq. (1), the magnetic flux efficiency shown in Eq. (2) and (3), and the energy gain shown in Eq. (4) and (5). These latter two quantities are interrelated through the parameter alpha.

Both large and small generators perform better with larger wire size or larger conductors, in general. This is due to the reduction of current densities on the conductors, with an associated reduction in magnetic flux loss. Though it is not generally understood, the small and large generators both perform better with round wire, rather than square wire. Also, all FCGs exhibit better performance as the inductive loading increases.

In two areas, the smaller FCGs show somewhat different characteristics from the larger generators. The first of these is the realized experimental gain, relative to the ideal gain of the unit. The small generators tested to date appear to be limited to current gains of a few ten's, at most. This result is reflected in the lower alpha parameters that have been measured for these FCGs. Another difference is that higher current loading in the small generators tend to show improved performance figures of merit until current saturation effects become significant. We have speculated that this may be due to a better connection being formed between the armature and stator, perhaps due to higher internal voltages.

Manuscript received August 1, 2003

References

[1] Fowler C.M., Caird C.S., and Garn W.B. An Introduction to Explosive Magnetic Flux Compression Generators // Los Alamos Scientific Laboratory, Report LA-5890-MS. – 1975, March.

[2] Grover J.E., Stutzer O.M., and Johnson J.L. // Small Helical Flux Compression Amplifiers // in Proc. Second International Conference on Megagauss Magnetic Field Generation and Related Topics. – 1979. – P. 163.

[3] Freeman B.L., Boydston J.C., Ferguson J.M., Lindeburg B.A., Luginbill A.D. and Tutt T.E., "Development of Small, Tapered Stator Helical Magnetic Flux Compression Generators // in Proc. 14th IEEE International Pulsed Power Conference. – 2003.

[4] Stuetzer O.M. "Theory of Small Compressed Magnetic Flux Current Amplifiers // Sandia Laboratories Technical Report, SAND79-1075. – 1979, May.

[5] Abe D.K. and Chase J.B. Experiments with Small Helical Flux Compression Generators – P. 405–409.

[6] Abe D.K. and Chase J.B., Comparison of Numerical Helical Generator Simulations with Experimental Results. – P. 411–416.

[7] Chase J.B. CIRC: A Specialized Circuit Analysis Computer Simulation Program for a High Explosive Generator Model – P. 397 – 403.

[8] Prishchepenko A.B. private communications.

[9] Demidov V.A., Boriskin A.S., Dimant E.M., Kazakov S.A., Ionov V.A., Shapovalov E.V., and Yanenko V.A. Study of Fast Compact Helical MCG – P. 913–916.

[10] V.A. Demidov, V.D. Sadunov, S.A. Kazakov, L.N. Plyashkovich, T.V. Trischenko, S.N. Golosov, A.V. Blinov, I.K. Fetisov, M.V. Korotchenko, and Ye.V. Shapovalov, "Helical Cascade FCG Powered by Piezogenerator", pp. 1476 - 1481 (19

[11] Brooker C.J., Manton N.H., and McKay N., Helical Flux Compressor Development for Compact Pulsed Power Sources // Megagauss Magnetic Field Generation and Power Applications. – 1994. – P. 511–517.

[12] Smith I.R., private communication.

[13] Holt T., Neuber A., Dickens J. and Kristiansen M. Impact of Helix Geometry on MCG Flux Losses // IEEE – P. 905–908.

[14] Neuber A.A., Hernandez J., Holt T.A., Dickens J.C., and Kristiansen M. Physical Efficiency Limits of Inch-Sized Helical MFCG's // IEEE

[15] Fowler C.M. and Caird R.S. The Mark IX Generator // in Proc. 7th IEEE Pulsed Power Conference. – 1989. – P. 475.

Table 3. TTU generators (courtesy of A. Neuber, TTU)

Generator	Geometry	Armature OD (mm)	Stator ID (mm)	Stator Length (mm)	Number of Turns	Stator Wire	Input Field/ Current	Peak Current (A)	α	Current Gain	Energy Gain
TTU I	SINGLE HELIX WIRE	38.1	66	102	32	Magnet Wire	96	5083	0.6516	52.9513889	6.339892565
TTU I	SINGLE HELIX WIRE	38.1	66	102	32	N.I. AWG12	13	763	0.6684	58.6538462	7.778935634
TTU I	SINGLE HELIX WIRE	38.1	66	102	32	N.I. Electric Wire	910	57550	0.6659	63.2417582	7.894471709
TTU I	SINGLE HELIX WIRE	38.1	66	102	32	Square Magnet Wire	885	55500	0.6620	62.7118644	7.579309379
TTU I	SINGLE HELIX WIRE	38.1	66	102	32	Russian Wire	950	25500	0.5396	26.8421053	1.621121884
TTU I	SINGLE HELIX WIRE	38.1	66	102	32	Electric Wire (With Insulation)	870	64400	0.7022	74.0229885	11.92792509
TTU I	SINGLE HELIX WIRE	38.1	66	102	32	Square Magnet Wire	895	60740	0.6772	67.8659218	9.091147539
TTU I	SINGLE HELIX WIRE	38.1	66	102	32	Triple Helix (Magnet Wire – Polyimide)	385	38000	0.7283	98.7012987	17.79853601
TTU I	SINGLE HELIX WIRE	38.1	66	102	16	Double Helix (Polyester heavy build)	3	190	0.6809	65.5172414	9.226369168
TTU I	SINGLE HELIX WIRE	38.1	66	102	16	Double Helix (TFE Teflon – Tin coating)	396	31000	0.7086	78.2828283	13.0309865
TTU II	SINGLE HELIX WIRE	38.1	89	102	32	Electric Wire	875	78000	0.6949	89.1428571	12.41632653
TTU II	SINGLE HELIX WIRE	38.1	89	102	32	Fluoroelastomer Heat Shrink Tubing	820	47500	0.6369	57.9268293	5.727642875
TTU II	SINGLE HELIX WIRE	38.1	89	102	32	Formvar	95	4400	0.6018	46.3157895	3.659708741
TTU II	SINGLE HELIX WIRE	38.1	89	102	16	Double Helix (Electric Wire)	541	31000	0.7962	57.3012939	20.32604651
TTU III	SINGLE HELIX WIRE	38.1	66	51	32	Single Helix (TFETeflon – Tin Coating)	24	1373	0.6365	57.6890756	5.69317397
TTU IV	SINGLE HELIX WIRE	15.9	28.7	27.9	30	Magnet Wire (30 turns)	45	982	0.5826	21.7660093	2.395411489
TTU IV	SINGLE HELIX WIRE	15.9	28.7	27.9	30	Magnet Wire (30 turns)	21	358	0.5481	16.8075117	1.640278747
TTU V	SINGLE HELIX WIRE	15.9	28.4	22.9	20	PVC Insulated AWG 22	93	1225	0.6857	13.172043	4.040474233
TU VI	TAPERED HELIX	38.1	66	130	32+	AWG 12 Electric Wire	501	79897	0.7198	159.551881	22.14741841

Table 4. TAMU generator

Generator	Geometry	Armature OD (mm)	Stator ID (mm)	Stator Length (mm)	Number of Turns	Stator Wire	Input Field/ Current	α	Current Gain	Energy Gain
Mark I	Cylindrical, 2 Det.	1.27		2.54	16	# 14 Magnet	12 kg	–		
Mark IIa	Cylindrical, 2 Det.	0.9525	1.905	5.08	29	# 14 Magnet	216/280 A	0.418/0/442	8.94/6.00	0.43/0.91
Mark IIb	Cylindrical, 1 Det.	0.9525	1.905	5.08	36	# 16 Magnet	204/170 A	0.349/0.417	7.50/6.49	0.15/0.30
Mark III	Cylindrical, 1 Det.	0.947	1.905	5.08	29	# 14 Magnet	4.020-4.280 A	0.359-0.581	3.87-8.03	0.26-1.61
Mark IIIa	Cylindrical, 1 Det.	0.947	1.905	5.08	23	# 12 Magnet	632 A	0.581	6.05	1.65
Mark IIIb	Cylindrical, 1 Det.	0.947	1.905	5.265	13.75	# 24 Kapton	672 A	0.412	3.42-5.25	0.49-1.12
Mark IV	Cylindrical, 1 Det.	0.947	1.905	5.08	29	# 14 Magnet	780/792 A	0.388/0.494	5.37/4.43	0.38/0.97
Mark V	Cylindrical, 1 Det.	2.54	4.66	6.96	40/41	# 14 Magnet	124/110 A	0.618/0.505	40.52/32.39	4.13/1.07
Mark Va	Cylindrical, 1 Det.	2.41	4.57	6.96	18	# 12 Magnet	371/734 A	0.479/0.422	9.31/7.45	0.82/0.48
Mark Vc	Cylindrical, 1 Det.	2.54	5.08	7.71		# 24 Kapton	99.2	0.441	10.23	0.53
Mark Vd	Cylindrical, 1 Det.	2.54	5.08	7.71		# 16 Magnet	880 A	0.596	11.46	2.20
Mark 100	10 Tapered, 1 Det.	2.54	5.02-2.56	6.985	29	# 14 Magnet	9.436/9.817 A	0.655/0.648	7.40/7.52	2.58/2.51
Mark 100a	10 Tapered, 1 Det.	2.54	5.02-2.65	6.985	27	# 12 Magnet	7.224/7.060 A	0.629/0.631	8.04/8.37	2.35/2.42
Mark 101	12 Tapered, 1 Det.	2.54	5.53-2.65	6.985	31	# 12 Round	10.147-11.310 A	0.475-0.666	6.52-10.97	0.82-3.15
Mark 101a	12 Tapered, 1 Det.	2.69	5.53-2.65	6.985	33	# 12 Round	1008 A	0.693	13.59	3.11
Mark 101b	12 Tapered, 1 Det.	2.69	5.644-3.005	6.985	41	# 14 Round	1032/3000 A	0.604/5.31	16.34/11.68	2.62/1.33
Mark 102	Cyldrical+ 10 Tapered, 1 Det.	2.54	5.53-2.65	6.985	44	# 12 Round	896/934 A	0.483/0.480	12.35/8.01	0.84/0.84
Mark 103	13 Tapered, 1 Det.	2.54	5.64-3.00	6.53	38	# 14 Round	992/912 A	0.604/0.497	16.47/22.73	2.62/0.96